65th International Astronautical Congress, Toronto, Canada.

IAC-14-C1.8.6

A HOMOTOPY-BASED METHOD FOR OPTIMIZATION OF HYBRID HIGH-LOW THRUST TRAJECTORIES

Nicola Sullo
School of Engineering, University of Glasgow, Glasgow, United Kingdom
n.sullo.1@research.gla.ac.uk

Matteo Ceriotti
School of Engineering, University of Glasgow, Glasgow, United Kingdom
matteo.ceriotti@glasgow.ac.uk

Space missions require increasingly more efficient trajectories to provide payload transport and mission goals by means of lowest fuel consumption, a strategic mission design key-point. Recent works demonstrated that the combined (or hybrid) use of chemical and electrical propulsion can give important advantages in terms of fuel consumption, without losing the ability to reach other mission objectives: as an example the Hohmann Spiral Transfer, applied in the case of a transfer to GEO orbit, demonstrated a fuel mass saving between 5-10% of the spacecraft wet mass, whilst satisfying a pre-set boundary constraint for the time of flight. Nevertheless, methods specifically developed for optimizing space trajectories considering the use of hybrid high-low thrust propulsion systems have not been extensively developed, basically because of the intrinsic complexity in the solution of optimal problem equations with existent numerical methods. The study undertaken and presented in this paper develops a numerical strategy for the optimization of hybrid high-low thrust space trajectories. An indirect optimization method has been developed, which makes use of a homotopic approach for numerical convergence improvement. The adoption of a homotopic approach provides a relaxation to the optimal problem, transforming it into a simplest problem to solve in which the optimal problem presents smoother equations and the shooting function acquires an increased convergence radius: the original optimal problem is then reached through a homotopy parameter continuation. Moreover, the use of homotopy can make possible to include a high thrust impulse (treated as velocity discontinuity) to the low thrust optimal control obtained from the indirect method. The impulse magnitude, location and direction are obtained following from a numerical continuation in order to minimize the problem cost function. The initial study carried out in this paper is finally correlated with particular test cases, in order to validate the work developed and to start investigating in which cases the effectiveness of hybrid-thrust propulsion subsists.

I. INTRODUCTION

Since the beginning of space exploration one of the most important mission requirements has consisted in designing the spacecraft so that it could be as light as possible. The reasons for this are found in the necessity to make the mission physically possible as well as to reduce the costs related in launching and propelling a spacecraft in space.

Specific studies have been carried out during the last decades with the intent to improve methods for designing space trajectories minimizing the fuel consumption. These studies have exploited in particular astrodynamics and space propulsion. Astrodynamics research has made possible, in fact, to study how to optimally propel a spacecraft through impulsive manoeuvres provided by a chemical thruster, how to make advantage of gravity assists for interplanetary missions and how to propel a spacecraft by means of optimal controlled continuous thrust. The research carried out in the astrodynamics field has also driven the developments related to the technological side of space propulsion. Novel and more efficient propulsion systems have been studied and developed like, for example, the class of electrical thrusters that, thanks to their higher specific impulse, are generally more efficient than chemical thrusters. Anyway, specific optimization studies must always be conducted in order to obtain optimal-fuel transfers trajectories that can benefit of the novel propulsion systems developed, or efficiently use the traditional propulsion systems (e.g. chemical thrusters).

Since the beginning of space exploration, the earliest trajectory optimization studies were related to the design of optimal space trajectories with impulsive high-thrust manoeuvres that are provided by the conventional chemical thrusters, the first class of thrusters to be introduced in space propulsion. Subsequently electrical thrusters, which provide a low but continuous thrust, were developed and studies to find solutions for fuel-optimal low-thrust trajectories began to be carried out.

Currently a new frontier in space exploration consists in the use of variable specific impulse electric thruster (VASIMR) that are able to bring increased advantages especially in terms of fuel mass consumption if compared to other electric thrusters[1-3].

Hybrid high-low thrust propulsion pushes to the limit the concept of variable specific impulse thrusters. This type of propulsion is realized by supplying the spacecraft with a dual propulsion system consisting in a chemical (high thrust) and an electrical (low thrust) thruster. The aim of hybrid thrust propulsion is to obtain as final goal a benefit in terms of the overall spacecraft mass reduction respect to use only an electric engine, even if a dual propulsion system must be mounted aboard the spacecraft.

Optimization studies must be carried out in order to make an efficient use of the propulsion systems provided.

In particular, in regard to the optimization of low-thrust trajectories, mainly three different classes of optimization methods are used in literature[4-7]: the class of direct methods[4], the indirect methods[5] and global optimization techniques[7]. Direct methods attempt to find an optimal solution by iteratively minimizing the problem cost function until a minimum is found. Indirect methods, instead, seek for an optimal solution by solving the optimality conditions analytically derived for the specific problem studied. Direct and indirect methods generally seeks for optimal local solutions (local minima); global methods, unlike the previous two methods, are so called because they attempt to find a global optimal solution; moreover they can manage more complex and/or not regular objective functions and constraints, that can be numerically difficult or not possible to solve with direct or indirect methods.

Noteworthy aspects in space trajectory optimization and typical of indirect methods consist in the fact that the latter:

(a) are more precise and generally faster in finding a solution than other optimization techniques;

(b) do not require any first assumptions regarding the structure of the control.

However their main drawback[8-10] is that the convergence radius for the solution of the fuel-optimal problem with current numerical solvers is typically narrow, and this implies that a good initial guess is needed in order to solve the problem satisfying the optimality conditions.

For this reason, relaxation techniques have been studied in order to reduce the problem stiffness and increase the convergence radius. One of the most used in literature, especially in Earth and interplanetary low-thrust transfers, is the relaxation technique based on the combined use of homotopy and numerical continuation[8-10]. Using this technique and by means of homotopy it has been possible to link the fuel-optimal problem solution to the energy-optimal problem solution that it is easier to obtain, basically because of an increased convergence radius of the solution search space. Next, the relaxed optimal problem (the energy-optimal problem) is brought back to the original optimization problem by means of numerical continuation technique that, starting from the energy-optimal problem solution and by means of an iterative process, finds the solution to optimal control problems progressively closer to the fuel-optimal problem until the solution for this problem is finally achieved.

Although low-thrust transfers provide important advantages regarding fuel mass saving, recent investigations[11-14] have already proven that the use of hybrid high-low thrust propulsion systems for space transfers can provide a further gain in terms of fuel mass expended.

A noteworthy study to be mentioned applies hybrid-thrust propulsion to an Earth to Moon transfer in which the complex n-body dynamics due to the Sun-Earth-Moon system is also considered and exploited[11-13]. The hybrid-thrust trajectory basically consists of a first ballistic portion in which the spacecraft is injected into an Earth escape trajectory by means of an impulsive manoeuvre performed by a chemical thruster; subsequently the spacecraft is captured on the moon target orbit by means of its low-thrust propulsion system. Following from an optimization of the hybrid-thrust transfer trajectory, it has been possible to outperform the fuel mass consumption from a single-propulsion solution, thus demonstrating the effectiveness of hybrid-thrust propulsion.

Further studies have been conducted in the Hohmann Spiral Transfer[14], a particular type of transfer composed by a Hohmann impulsive manoeuvre from the departing orbit followed by a spiral (low thrust) trajectory arriving to the final target orbit. The study showed an application to a transfer from a Low Earth Orbit (LEO) to a Geostationary Earth Orbit (GEO) and, following an optimization of the hybrid-thrust trajectory it demonstrated a fuel mass saving between 5-10% of the spacecraft wet mass, whilst satisfying a pre-set boundary constraint for the time of flight.

However, methods developed so far to design and optimize hybrid thrust transfer trajectories are based on patching together a low-thrust trajectory stretch with one obtained from an impulsive high-thrust manoeuvre. Subsequently an optimization is carried out in order to outperform the high or low thrust solutions. Furthermore these studies have proven the effectiveness of hybrid-thrust propulsion in specific application cases only.

The purpose of this work is to set up a framework for a general optimization of hybrid thrust trajectories: in the current paper a preliminary work is presented and results discussed.

The paper is organized in three main sections: section II in which the fuel-optimal low-thrust problem is stated, the homotopic transformations are introduced and finally the impulsive manoeuvre inclusion is explained; section III in which the numerical techniques and algorithms to solve the hybrid-thrust optimal problem are described; finally in section IV the numerical test case is presented and in section V the preliminary results are analysed and discussed.

II. ANALYTICAL MODEL

II.I Fuel-optimal low-thrust problem statement

The dynamical model used is based on the two-body problem with a perturbing acceleration[15,16]:

$$\ddot{\boldsymbol{r}} = -\frac{\mu}{r^3}\boldsymbol{r} + \boldsymbol{a}_P \qquad [1]$$

with $\boldsymbol{r}$ the spacecraft position vector, μ the Earth's gravitational parameter and $\boldsymbol{a}_P$ the perturbing acceleration due to low-thrust.

The dynamics equation above is formulated making use of Cartesian coordinates. However Cartesian coordinates cannot be convenient in terms of numerical stability for computer simulations, this for possible strong oscillations in the variables of the dynamics equations[8,9].

A different set of coordinates to express the dynamics equations consists in the Modified Equinoctial Elements (MEE)[17,18]. The MEE completely define the position of an object on an orbit in the phase space (position and velocity) and, moreover, present non-singular equations of motion. They are defined as follows:

$$\boldsymbol{x} = \begin{bmatrix} p \\ f \\ g \\ h \\ k \\ L \end{bmatrix} = \begin{bmatrix} a(1-e^2) \\ e\cos(\omega+\Omega) \\ e\sin(\omega+\Omega) \\ \tan\left(\frac{i}{2}\right)\cos(\Omega) \\ \tan\left(\frac{i}{2}\right)\sin(\Omega) \\ \Omega+\omega+\nu \end{bmatrix} \qquad [2]$$

where a is the semi-major axis, e the eccentricity, i the inclination, Ω the right longitude of ascending node, ω the argument of perigee and ν the true anomaly.

In this work the coordinates set given by MEE are used and, therefore, the dynamics equation [1] is derived in the MEE set: in order to proceed to this derivation it is first necessary to introduce the orbital reference frame in which the components of the perturbing acceleration due to the thrust are expressed. This reference frame is represented in Fig. 1 and its components are centred in the spacecraft and are defined as $(\boldsymbol{c}_1, \boldsymbol{c}_2, \boldsymbol{c}_3)$, where $\boldsymbol{c}_1$ is the radial unit vector zenith pointing, $\boldsymbol{c}_2$ is the transverse unit vector in the orbit plane pointing towards the orbit's rotation direction and $\boldsymbol{c}_3$ the normal unit vector pointing in the same direction and versus of the orbit's angular momentum.

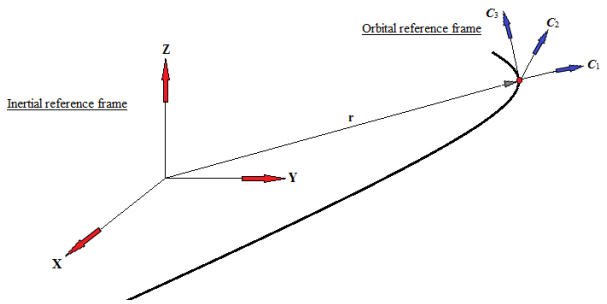

Fig. 1: Inertial reference system and orbital reference frame.

By considering the additional equation describing the spacecraft mass variation due to fuel consumption, the dynamics equations are thus expressed as follows[8,9]:

$$[\dot{\boldsymbol{y}}] = \begin{bmatrix} \dot{\boldsymbol{x}} \\ \dot{m} \end{bmatrix} = \begin{bmatrix} \left(\frac{T_{max}}{m}\right)\boldsymbol{B}\cdot\boldsymbol{u} + \boldsymbol{a} \\ -\frac{T_{max}}{(lt)_{I_{sp}}g_0}\|\boldsymbol{u}\| \end{bmatrix} \qquad [3]$$

with

$$\boldsymbol{B} = \begin{bmatrix} 0 & \frac{2p}{q}\sqrt{\frac{p}{\mu}} & 0 \\ \sqrt{\frac{p}{\mu}}\sin(L) & \sqrt{\frac{p}{\mu}}\frac{1}{q}[(q+1)\cos(L)+f] & -\sqrt{\frac{p}{\mu}}\frac{g}{q}[h\sin(L)-k\cos(L)] \\ -\sqrt{\frac{p}{\mu}}\cos(L) & \sqrt{\frac{p}{\mu}}\frac{1}{q}[(q+1)\sin(L)+g] & \sqrt{\frac{p}{\mu}}\frac{f}{q}[h\sin(L)-k\cos(L)] \\ 0 & 0 & \sqrt{\frac{p}{\mu}}\frac{s^2\cos(L)}{2q} \\ 0 & 0 & \sqrt{\frac{p}{\mu}}\frac{s^2\sin(L)}{2q} \\ 0 & 0 & \sqrt{\frac{p}{\mu}}\frac{1}{q}[h\sin(L)-k\cos(L)] \end{bmatrix}$$

$$\boldsymbol{a} = \begin{bmatrix} 0 & 0 & 0 & 0 & 0 & \sqrt{\mu p}\left(\frac{q}{p}\right)^2 \end{bmatrix}^T$$

$$\boldsymbol{u} = [u_1 \quad u_2 \quad u_3]^T$$

and

$$q = 1 + f\cos(L) + g\sin(L)$$

$$\chi = \sqrt{h^2 + k^2}$$

$$s^2 = 1 + \chi^2$$

In the above relationships m is the spacecraft mass, $\boldsymbol{u}$ the normalized control vector expressed in $(\boldsymbol{c}_1, \boldsymbol{c}_2, \boldsymbol{c}_3)$, T_{max} the maximum low thrust magnitude, ${}^{(lt)}I_{sp}$ the low thrust specific impulse, g_0 the standard gravitational acceleration.

The low thrust optimal fuel mass consumption problem can be therefore stated as follows[8-10]:

$$\mathcal{P}\begin{cases} \min \int_{t_0}^{t_f} \|\boldsymbol{u}\| dt \\ \dot{\boldsymbol{y}} = f(t, \boldsymbol{x}(t), \boldsymbol{u}(t)) \\ t_0 = fixed\,, \boldsymbol{y}(t_0) = \boldsymbol{y}_0 \\ t_f = fixed \\ \boldsymbol{y}(t_f) = [p_f \quad f_f \quad g_f \quad h_f \quad k_f \quad free \quad free]^T \end{cases}$$

According to the Pontryagin Minimum Principle, the solution of the optimal control problem above shown is obtained by minimizing the augmented cost function J':

$$J' = \boldsymbol{\xi} \cdot \boldsymbol{\varphi}\left(t_f, \boldsymbol{x}(t_f)\right) + \int_{t_0}^{t_f} \mathcal{L}\, dt \qquad [4]$$

where $\boldsymbol{\xi}$ represents the Lagrange multiplier for the punctual cost function, $\boldsymbol{\varphi}$ the boundary conditions at the final time and $\mathcal{L} = \|\boldsymbol{u}\|$ the Lagrangian.
Following from the theory and the related literature[8-10], the conditions derived as a solution for the optimal problem stated are expressed as integral and punctual conditions. The integral conditions are the state and costates equation and the optimal control, the last derived by minimizing the Hamiltonian

$$\mathcal{H} = \mathcal{L} - \langle \boldsymbol{\lambda}\,, \dot{\boldsymbol{y}} \rangle = \left(1 - \frac{T_{max}}{{}^{(lt)}I_{sp} g_0} \lambda_m\right) \|\boldsymbol{u}\| + \frac{T_{max}}{m} \left(\langle \boldsymbol{B} \cdot \boldsymbol{u}\,, \boldsymbol{\lambda}_x \rangle + \langle \boldsymbol{a}\,, \boldsymbol{\lambda}_x \rangle\right) \qquad [5]$$

with $\boldsymbol{\lambda} = [\boldsymbol{\lambda}_x \quad \lambda_m]^T$ and $\boldsymbol{\lambda}_x = [\lambda_p \quad \lambda_f \quad \lambda_g \quad \lambda_h \quad \lambda_k \quad \lambda_L]^T$ and λ_m are respectively the costates relative to the MEE and the spacecraft mass. The optimal control $\boldsymbol{u}^*$ is therefore given by the well-known bang-bang law given by:

$$\begin{cases} \boldsymbol{u}^* = -\frac{\boldsymbol{B}^T \cdot \boldsymbol{\lambda}_x}{\|\boldsymbol{B}^T \cdot \boldsymbol{\lambda}_x\|} & if\ \psi < 0 \\ \boldsymbol{u}^* = -\alpha \frac{\boldsymbol{B}^T \cdot \boldsymbol{\lambda}_x}{\|\boldsymbol{B}^T \cdot \boldsymbol{\lambda}_x\|} & if\ \psi = 0 \\ \boldsymbol{u}^* = \boldsymbol{0} & if\ \psi > 0 \end{cases} \qquad [6]$$

with the scalar $\alpha \in [0,1]$, and the switching function ψ defined as

$$\psi = 1 - \frac{T_{max}}{{}^{(lt)}I_{sp} g_0} \lambda_m - \frac{T_{max}}{m} \|\boldsymbol{B}^T \cdot \boldsymbol{\lambda}_x\| \qquad [7]$$

The costates equations, instead, are given by the following relationship:

$$\dot{\boldsymbol{\lambda}} = -\frac{\partial \mathcal{H}}{\partial \boldsymbol{x}} \qquad [8]$$

The punctual conditions for optimality correspond to the transversality conditions defined as follows:

$$\begin{cases} \lambda_L(t_f) = 0 \\ \lambda_m(t_f) = 0 \end{cases} \qquad [9]$$

The solution of optimal control problems is commonly obtained through multiple shooting or single shooting methods[4]. The single shooting method, adopted here[8-10], transforms the optimization problem into the direct solution of a system of nonlinear equations $\boldsymbol{S}(\boldsymbol{z}) = \boldsymbol{0}$, that for the current problem is:

$$\boldsymbol{S}(\boldsymbol{z}) = \begin{Bmatrix} p(t_f) - p_f \\ f(t_f) - f_f \\ g(t_f) - g_f \\ h(t_f) - h_f \\ k(t_f) - k_f \\ \lambda_L(t_f) \\ \lambda_m(t_f) \end{Bmatrix} = \boldsymbol{0} \qquad [10]$$

with $\boldsymbol{z} \in \mathbb{R}^n$ the unknowns vector and $\boldsymbol{S} \in \mathbb{R}^m$ the so-called shooting function, i.e. a vector consisting of the left hand side of the system of m nonlinear equations. In the optimal control problem analysed here, the n unknowns are represented by the initial values of the costates; the m nonlinear equations are represented by the final state defects equations $\boldsymbol{x}(t_f) - \boldsymbol{x}_f = \boldsymbol{0}$ and the transversality conditions above mentioned. The final state defects equations make possible to satisfy the dynamics equations, integrated using the optimal control $\boldsymbol{u}^*$ previously shown and with the prescribed final state conditions; the transversality conditions are, again, the optimal punctual conditions derived by the Pontryagin Minimum Principle. So the fuel-optimal low-thrust problem is completely defined and ready to be numerically solved.

II.II Homotopy-based relaxation method

The shooting function solution for the optimal problem $\mathcal{P}$ is particularly tricky to obtain, because of

the numerical problems due to nonsmoothness and discontinuities in the differential equations defining the optimal problem. For this reason, current numerical solvers typically present a narrow convergence radius for the shooting function, so that a numerical solution is really hard or even impossible to obtain.

To overcome this problem, a homotopy-based relaxation method is resumed from literature[8-10] and here used.

Considering two continuous functions $\boldsymbol{f}$ and $\boldsymbol{g}$ defined respectively on the spaces $\boldsymbol{X}$ and $\boldsymbol{Y}$, an homotopy is defined[19] as a continuous function $\boldsymbol{H}: \boldsymbol{X} \times [0,1] \rightarrow \boldsymbol{Y}$ and such that $\forall \boldsymbol{x} \in \boldsymbol{X}$ $\boldsymbol{H}(\boldsymbol{x}, 0) = \boldsymbol{f}(\boldsymbol{x})$ and $\boldsymbol{H}(\boldsymbol{x}, 1) = \boldsymbol{g}(\boldsymbol{x})$.
In the fuel-optimal problem the (convex) homotopy transformation criterion is adopted in order to transform the Lagrangian of $\mathcal{P}$ as follows:

$$\mathcal{L} = \mathcal{L}_{mc} = \|\boldsymbol{u}\| \rightarrow \mathcal{L}_{H1} = \varepsilon_1 \|\boldsymbol{u}\| + (1 - \varepsilon_1)\|\boldsymbol{u}\|^2 \quad [11]$$

When $\varepsilon_1 = 1$ then $\mathcal{L} = \mathcal{L}_{mc}$, when instead $\varepsilon_1 = 0$ then $\mathcal{L} = \mathcal{L}_{ec} = \|\boldsymbol{u}\|^2$ that is the Lagrangian for the energy-optimal problem.
Following from [11], the shooting function of $\mathcal{P}$ is transformed in the homotopy

$$\boldsymbol{S}(\boldsymbol{z}, \varepsilon_1): \mathbb{R}^n \times [0,1] \rightarrow \mathbb{R}^m \quad [12]$$

that links the original fuel-optimal control problem into a "relaxed" problem easier to solve, i.e. the energy-optimal control problem. In particular, the relaxed problem presents smooth equations and a smooth optimal control; moreover the solution search space is increased.

The energy optimal problem is firstly solved by finding a solution to $\boldsymbol{S}(\boldsymbol{z}, 0) = \boldsymbol{0}$ and subsequently this solution is brought back to the fuel-optimal problem solution $\boldsymbol{S}(\boldsymbol{z}, 1) = \boldsymbol{0}$ by means of numerical continuation, as done in Ref.8-10.

Numerical continuation[20] is a technique used to solve parameterized systems of nonlinear equations $\boldsymbol{H}(\boldsymbol{x}, \varepsilon) = \boldsymbol{0}$ where commonly $\varepsilon \in [0,1]$. The numerical continuation algorithm accepts as input an initial solution to the parameterized system, generally in the form $[\boldsymbol{x}_0, 0]^T$ and gives as output a set of solutions $[\boldsymbol{x}_i, i]^T$ with $i \in [0,1]$ constituting the so called "zero path" that links $[\boldsymbol{x}_0, 0]^T$ with $[\boldsymbol{x}_1, 1]^T$.
Therefore it is possible to firstly solve $\boldsymbol{S}(\boldsymbol{z}, 0) = \boldsymbol{0}$ and thus obtain the energy-optimal problem solution $[\boldsymbol{z}_0, 0]^T$; subsequently this latter solution is given as input to the continuation algorithm that provides as final output $[\boldsymbol{z}_1, 1]^T$, i.e. the solution to the fuel-optimal control problem.

The new relaxed problem to solve via numerical continuation can now be stated as follows:

$$\mathcal{P}_{H1}\begin{cases} \min \int_{t_0}^{t_f} (\varepsilon_1 \|\boldsymbol{u}\| + (1 - \varepsilon_1)\|\boldsymbol{u}\|^2) dt \ , \ \ \varepsilon_1 \in [0,1] \\ \dot{\boldsymbol{y}} = f(t, \boldsymbol{x}(t), \boldsymbol{u}(t)) \\ t_0 = fixed \ , \boldsymbol{y}(t_0) = \boldsymbol{y}_0 \\ t_f = fixed \\ \boldsymbol{y}(t_f) = [p_f \quad f_f \quad g_f \quad h_f \quad k_f \quad free \quad free]^T \end{cases}$$

Here the optimal control $\boldsymbol{u}^*$ assumes the following smooth form:

$$\begin{cases} \boldsymbol{u}^* = -\frac{\boldsymbol{B}^T \cdot \boldsymbol{\lambda}_x}{\|\boldsymbol{B}^T \cdot \boldsymbol{\lambda}_x\|} & if \ \ \psi < -(1 - \varepsilon_1) \\ \boldsymbol{u}^* = \left(\frac{\psi}{2(1-\varepsilon_1)} - \frac{1}{2}\right) \frac{\boldsymbol{B}^T \cdot \boldsymbol{\lambda}_x}{\|\boldsymbol{B}^T \cdot \boldsymbol{\lambda}_x\|} & if \ \ |\psi| \leq (1 - \varepsilon_1) \\ \boldsymbol{u}^* = \boldsymbol{0} & if \ \ \psi > (1 - \varepsilon_1) \end{cases} \quad [13]$$

Despite the homotopy based relaxation method above mentioned, the solution to the energy optimal problem can still be hard to obtain if the low thrust maximum acceleration is below a certain value[8,9].

For this reason it can be necessary to introduce a second relaxation to the energy-optimal problem that makes it possible to find an easier solution. This additional relaxation is introduced making use of a second homotopy transformation based on the following fact[8,9]: if the departing and arriving orbits coincide and the final longitude is free, then the optimal control is identically equal to zero. The trivial and unique solution to the energy-optimal problem consists of a vector of zeros as the initial value for the costates:

$$\boldsymbol{z} = [0 \quad 0 \quad 0 \quad 0 \quad 0 \quad 0 \quad 0]^T$$

The new optimal problem to solve via numerical continuation, necessary to find the energy-optimal problem solution and thus to initialize the continuation relative to $\mathcal{P}_{H1}$, is defined as follows:

$$\mathcal{P}_{H0}\begin{cases} \min \int_{t_0}^{t_f} \|\boldsymbol{u}\|^2 dt \\ \dot{\boldsymbol{y}} = f(t, \boldsymbol{x}(t), \boldsymbol{u}(t)) \\ t_0 = fixed \ , t_f = fixed \\ p(t_o) = (1 - \varepsilon_0) p(t_f) + \varepsilon_0 p(t_o) \\ f(t_o) = (1 - \varepsilon_0) f(t_f) + \varepsilon_0 f(t_o) \\ g(t_o) = (1 - \varepsilon_0) g(t_f) + \varepsilon_0 g(t_o) \\ h(t_o) = (1 - \varepsilon_0) h(t_f) + \varepsilon_0 h(t_o) \\ k(t_o) = (1 - \varepsilon_0) k(t_f) + \varepsilon_0 k(t_o) \\ L(t_f) = free \\ m(t_f) = free \end{cases}$$

where $\varepsilon_0 \in [0,1]$. When $\varepsilon_0 = 0$ the departing orbit is collapsed to the arrival orbit; when instead $\varepsilon_0 = 1$ the departing orbit assumes its pre-set shape.
Therefore, solving $\mathcal{P}_{H0}$ for $\varepsilon_0 = 0$ means to solve the energy-optimal problem along the arrival orbit, that admits the trivial solution previously stated.

As result of the two numerical continuations (the first relative to $\mathcal{P}_{H0}$, the other relative to $\mathcal{P}_{H1}$), the solution for the fuel-optimal problem is finally achieved.

A remark that is worth to underline consists in a second important advantage made possible by introducing the homotopy transformation in $\mathcal{P}_{H0}$. In fact, by using this "initialization" homotopy, the initial solution vector for the shooting function is already known a priori, in the hypothesis that the final longitude is always left free, as stated in $\mathcal{P}_{H0}$. If instead the final longitude is kept fixed, the shooting function admits a non-trivial solution that is, however, not too far from the zeros solution vector[8,9].

Since the analysis initially undertaken in the current work addresses a simple orbit rendezvous, which implies that the final longitude is left free, it is not necessary to explore the numerical values of this initial solution vector through alternative ways, for example via a heuristic search. This implies a not negligible advantage in terms of computational effort needed for the numerical simulations.

II.III From low to hybrid thrust: inclusion of impulsive manoeuvre

This step is accomplished by means of a homotopy transformation and numerical continuation related approach that performs the inclusion of a state (velocity and mass) discontinuity in a point along the low-thrust fuel-optimal trajectory previously obtained. The discontinuity is included by means of the following transformations at the instant of the impulsive manoeuvre:

$$\boldsymbol{v}(t_C^+) = \boldsymbol{v}(t_C^-) + \varepsilon_2 \Delta v_{max,HT} \widehat{\Delta \boldsymbol{v}} \qquad [14]$$

relative to the spacecraft velocity and

$$\Delta m_{HT} = m^-(t_C)\left(1 - e^{-\frac{\varepsilon_2 \Delta v_{max,HT}}{{}^{(ht)}I_{sp} g_0}}\right) \qquad [15]$$

obtained from the well-known Tsiolkovsky formula and relative to the spacecraft mass.
In the above relationships t_C denotes the time instant when the impulsive manoeuvre is performed, $\Delta v_{max,HT}$ represents the maximum allowable variation in velocity due to the impulsive manoeuvre, $\widehat{\Delta \boldsymbol{v}}$ is the unit vector of high thrust impulse, Δm_{HT} is fuel mass burned during impulsive manoeuvre and ${}^{(ht)}I_{sp}$ is the high thrust specific impulse.

Initially when $\varepsilon_2 = 0$ the jump in the spacecraft's velocity and mass is null and the transfer trajectory coincides with the only low-thrust solution. Next, the magnitude of the velocity change is progressively increased by means of an iteratively approach where at each step ε_2 is slightly increased and an optimal problem, regarding the maximization of the spacecraft final mass, is solved. The starting solution for each optimization step is the one obtained from the previous step. The above described iterative process terminates when the final spacecraft mass $m(t_f)$ is maximized: this means that a subsequent optimization step does not involve an improvement in terms of a further maximization of $m(t_f)$.

The third and last optimal problem to solve at each continuation step is now given by:

$$\mathcal{P}_{H2}\begin{cases} \max m(t_f) \\ t \in [t_0, t_C^-]\begin{cases} \min \int_{t_0}^{t_f} \|\boldsymbol{u}\| dt \\ \dot{\boldsymbol{y}} = f(t, \boldsymbol{x}(t), \boldsymbol{u}(t)) \\ t_0 = fixed\ , \boldsymbol{y}(t_0) = \boldsymbol{y}_0 \\ t_c = optimization\ variable \\ \boldsymbol{y}(t_C^-) = [free]_{(7\times 1)} \end{cases} \\ \cup \\ t \in [t_C^+, t_f]\begin{cases} \min \int_{t_C^+}^{t_f} \|\boldsymbol{u}\| dt \\ \dot{\boldsymbol{y}} = f(t, \boldsymbol{x}(t), \boldsymbol{u}(t)) \\ t_C = optimization\ variable \\ \boldsymbol{r}(t_C^+) = \boldsymbol{r}(t_C^-) \\ \boldsymbol{v}(t_C^+) = \boldsymbol{v}(t_C^-) + \varepsilon_2 \Delta v_{max,HT} \widehat{\Delta \boldsymbol{v}} \\ m(t_C^+) = m(t_C^-) - \Delta m_{HT} \\ t_f = fixed \\ \boldsymbol{y}(t_f) = [p_f \quad f_f \quad g_f \quad h_f \quad k_f \quad free \quad free]^T \end{cases} \end{cases}$$

The optimization variables for the problem $\mathcal{P}_{H2}$ are: (a) the costates $\boldsymbol{\lambda}(t_0)$ evaluated at the beginning of the transfer trajectory (b) the costates $\boldsymbol{\lambda}(t_C^+)$ evaluated at the instant t_C and relative to the low-thrust trajectory stretch after the impulsive manoeuvre, (c) the unit vector of high thrust impulse $\widehat{\Delta \boldsymbol{v}}$ and the time t_C at which the impulsive manoeuvre takes place.

It is necessary to underline that the optimization problem given by $\mathcal{P}_{H2}$ involves a re-optimization of the two low-thrust trajectory arcs, one before and the other after the impulsive manoeuvre: in fact the solution to $\mathcal{P}_{H2}: t \in [t_0, t_C^-]$ as well as the solution to $\mathcal{P}_{H2}: t \in [t_C^+, t_f]$ must be re-calculated in order to take into account the impulsive manoeuvre and maximize the final spacecraft mass. This is accomplished by considering $\boldsymbol{\lambda}(t_0)$ and $\boldsymbol{\lambda}(t_C^+)$ as optimization variables for the problem $\mathcal{P}_{H2}$.

Fig. 2 below represents the low-thrust fuel-optimal trajectory given by the continuous line and in dashed line the optimal hybrid-thrust trajectory obtained as final solution of $\mathcal{P}_{H2}$.

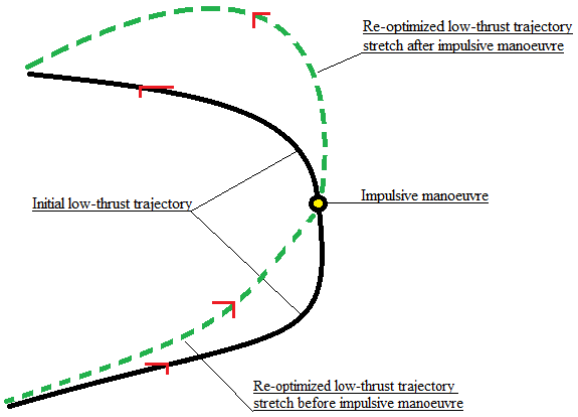

Fig.2: Low-thrust fuel-optimal trajectory (continuous line) and hybrid-thrust fuel-optimal trajectory (dashed line).

III. NUMERICAL SOLUTION

Summarizing the procedure elaborated so far for the hybrid-thrust trajectory optimization, it is so possible to split the latter in two phases: a first one in which a low-thrust fuel-optimal trajectory is obtained, a second one in which an impulsive manoeuvre is included and subsequent optimization steps are performed in order to optimize the total fuel mass consumption.

Specifically, the fuel-optimal low-thrust problem is firstly solved via indirect method and by means of two homotopic relaxation techniques applied in series: a first homotopy transformation turns the optimal-fuel low-thrust problem into an optimal-energy problem; a second homotopy transformation, in turn, leads to solve the optimal-energy transfer problem where the departing orbit is collapsed onto the arrival orbit and for which a (trivial) solution is already known. Starting from the latter problem a final solution for the optimal-fuel low-thrust case is reached by means of numerical continuation. Once a solution to the optimal low-thrust case is achieved, an impulsive manoeuvre is progressively included by means of a numerical continuation related approach performed on a third homotopy-based transformation. Each continuation step is solved by performing an optimization in which the spacecraft final mass is maximized. The optimal hybrid-thrust problem is solved once the magnitude of the impulsive manoeuvre is such to minimize the total fuel mass consumption.

The flow chart in Fig. 3 schematically summarizes the hybrid-thrust trajectory optimization framework.

The sub-sections below explain the fundamental aspects of the numerical implementation of the optimization method developed for hybrid-thrust trajectories.

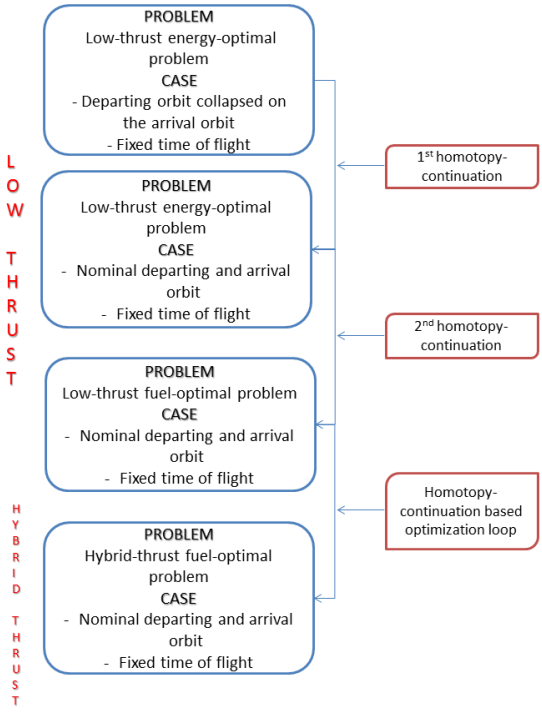

Fig.3: Flow chart for the hybrid-thrust trajectory optimization framework.

III.I Problem scaling

In order to have a numerically well-conditioned optimal problem and so improve the robustness of the code, it is necessary to introduce an appropriate scaling of the dimensional variables and the parameters involved in the optimization process.

Three different scaling sets have been developed in order to choose the more suited for the optimal transfer problem to be analysed. The first set, named LTM, has as physical quantities for scaling the length (L) of the departing orbit, the period (T) of the same departing orbit and spacecraft initial mass (M).

The second set, named LVM, uses as physical quantities for scaling the length (L) of the departing orbit, the tangential velocity (V) relative to a circular orbit having as radial length the length of the spacecraft departing position vector, the spacecraft initial mass (M).

Lastly the third set, named VTM, adopts as physical quantities for scaling the tangential velocity (V) relative to a circular orbit having as radial length the length of the spacecraft departing position vector, the period (T)

of the departing orbit and the spacecraft initial mass (M).

The three different sets have been tested in order to find the more suitable for the numerical simulations: however it has been found that the use of each one is almost equivalent to the use of the others. For the numerical test case simulated the LVM set has been chosen but, for the above mentioned reasons, no particular preference has been given in choosing this particular scaling set among the others.

III.II Discrete continuations

The numerical continuations relative to the problems $\mathcal{P}_{H0}$, $\mathcal{P}_{H1}$ and $\mathcal{P}_{H2}$ are implemented in the form of discrete continuations.

The numerical discrete continuation[8-10,20] algorithm used in this work consists in finding the zeros of $\boldsymbol{S}(\boldsymbol{z},\varepsilon)\colon \mathbb{R}^n \times \mathbb{R} \to \mathbb{R}^m$ for $\varepsilon = 1$ by starting to solve $\boldsymbol{S}(\boldsymbol{z},0)$ and then progressively increasing the scalar continuation parameter $\varepsilon \in [0,1]$ and finding, for each subsequent ε, the zeros of $\boldsymbol{S}(\boldsymbol{z},\varepsilon)$. The solution for $\boldsymbol{S}(\boldsymbol{z},\varepsilon)$ at the *i*-th step during discrete continuation is obtained using as initial guess (for the numerical solver) the solution at the (*i*-1)-th step.

An adaptive step size $\Delta\varepsilon$ for the continuation parameter has been implemented, in order to decrease the step size (using a halved step length) if the numerical solver does not find a solution at the *i*-th step, to increase the step size to speed up the continuation (using a doubled step length) if the numerical solver finds a solution at the *i*-th step.

The numerical solver used to solve the system of nonlinear equations, given by the shooting function, is the MATLAB *fsolve*.

III.III Impulsive manoeuvre inclusion and optimization

Initial guess

The impulsive manoeuvre needs, to be included, an initial guess for the 4 optimization variables given by the unit vector of high thrust impulse $\widehat{\Delta\boldsymbol{v}}$ (3 variables) and the time instant when the impulsive manoeuvre is performed t_C (1 variable).

Considering a quite small magnitude of the impulse when it is firstly included, any initial guess values provided for $\widehat{\Delta\boldsymbol{v}}$ and t_C must give a hybrid-thrust solution really close to the departing low-thrust fuel-optimal solution. For this reason, user's choice values can be entered in the optimization algorithm as initial guess for $\widehat{\Delta\boldsymbol{v}}$ and t_C.

Regarding the initial guess for the costates $\boldsymbol{\lambda}(t_0)$ and $\boldsymbol{\lambda}(t_C^+)$, the respective costate values resulting from the low-thrust fuel-optimal trajectory are provided as starting point for the third continuation.

Impulsive manoeuvre optimization

Once a first guess is provided, the last continuation is performed in order to optimize the hybrid-thrust trajectory and finding the final optimal impulsive manoeuvre, in terms of Δv magnitude and thrust direction, as well as time instant of the impulse. This approach, as already explained in the previous section, is accomplished by means of consecutive optimization iterations where, at each step, the final spacecraft mass is maximized. The optimization iterations are carried out through an algorithm based on a direct optimization method.

In this instance the algorithm used is the MATLAB *fmincon*, based on Sequential Quadratic Programming (SQP).

The objective function to be minimized by *fmincon* is simply given by the inverse of the spacecraft final mass: this means that the spacecraft final mass has to be maximized.

The nonlinear constraints imposed for *fmincon* are given by: (a) the final state defects equations $\boldsymbol{x}(t_f) - \boldsymbol{x}_f = \boldsymbol{0}$, (b) the condition regarding the fact that $\|\widehat{\Delta\boldsymbol{v}}\| = 1$.

IV. NUMERICAL TEST CASE

Software validation test case

In order to validate the optimization framework for hybrid-thrust trajectories developed so far, a test case have been numerically simulated and preliminary results are following shown and discussed.

The test case regards an interplanetary transfer from Earth to Mars orbit.

The time of flight is $ToF = t_f - t_0 = 450\ days$. The set of MEE for the initial and final spacecraft position are respectively:

$$\begin{cases} p_0 = 1.4960 \cdot 10^8\ km \\ f_0 = 0 \\ g_0 = 0 \\ h_0 = 0 \\ k_0 = 0 \\ L_0 = 0 \end{cases} \quad \text{and} \quad \begin{cases} p_f = 2.2595 \cdot 10^8\ km \\ f_f = 0.0854 \\ g_f = -0.0379 \\ h_f = 0.0105 \\ k_f = 0.0123 \\ L_f = free \end{cases}$$

The departing and arriving times are kept fixed and the true longitude at the arriving time of the transfer trajectory is left free.

The following problem parameters have been considered:

$m_0 = 1800\ kg$

$T_{max} = 0.5\ N$

$^{(lt)}I_{sp} = 4300\ s$

$^{(ht)}I_{sp} = 325\ s$

The high-thrust impulse initially included corresponds to an impulsive manoeuvre of $\Delta v = 10\ m/s$.

Results analysis

Following, the cases of energy-optimal, fuel-optimal and hybrid-thrust are illustrated in the plots for the transfer trajectory, optimal control and spacecraft mass. The evolution of the trajectory optimization progress is thus illustrated through the three homotopy-continuation steps.

Regarding the transfer trajectory evolution, it has been computed as follows:

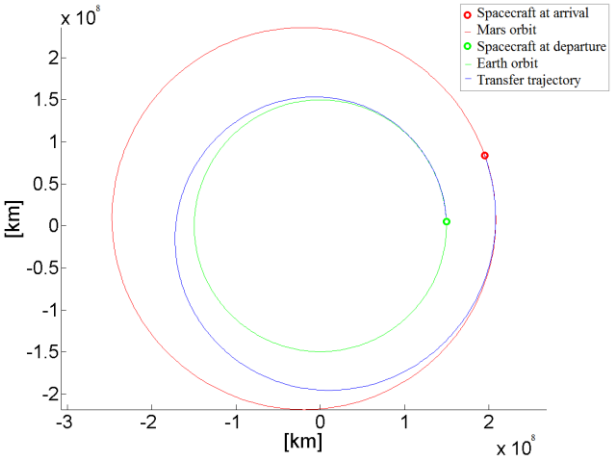

Fig.4: Spacecraft transfer trajectory from Earth to Mars in the energy-optimal case

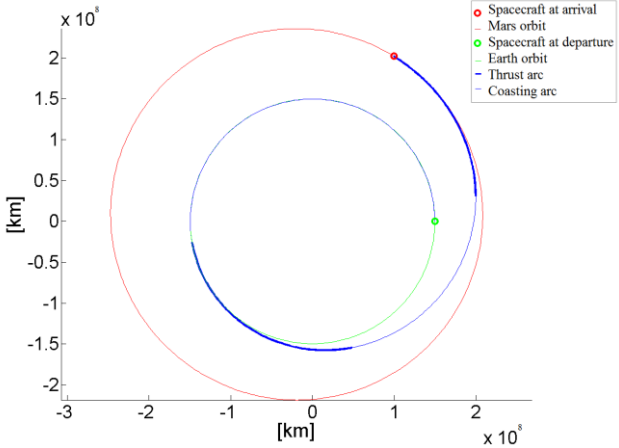

Fig.5: Spacecraft transfer trajectory from Earth to Mars in the fuel-optimal case

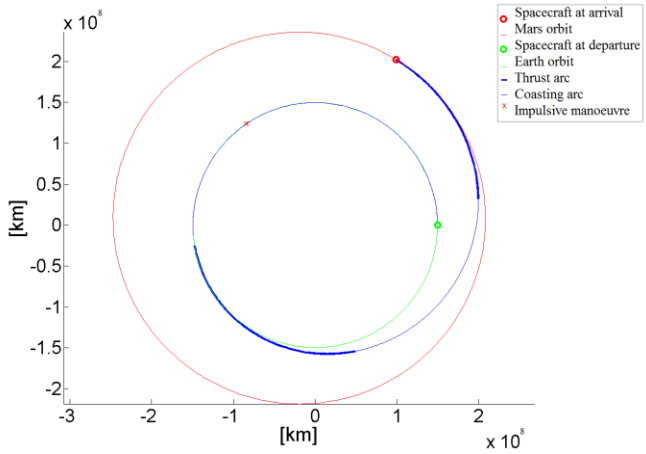

Fig.6: Spacecraft transfer trajectory from Earth to Mars in the hybrid high-low thrust case

The optimal control assumes the following evolution:

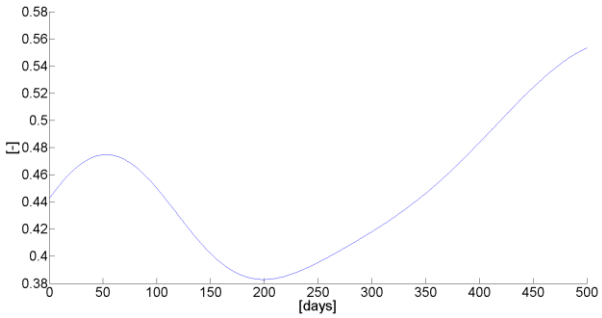

Fig.7: Normalized control vs time in the energy-optimal case

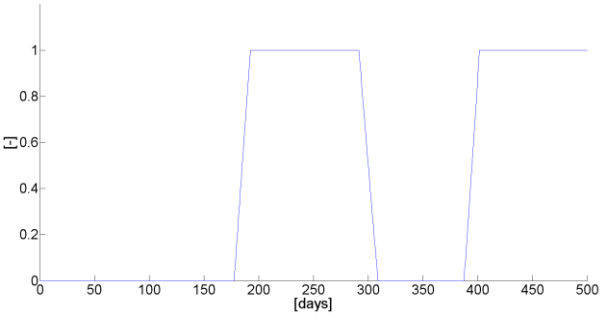

Fig.8: Normalized control vs time in the fuel-optimal case

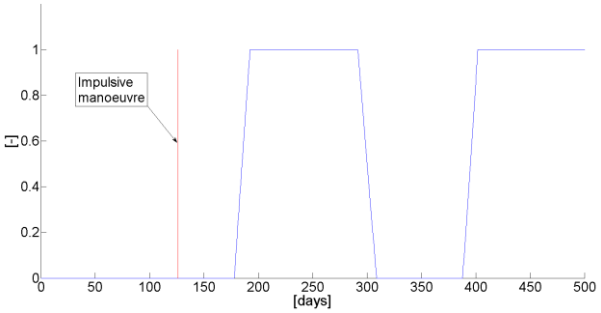

Fig.8: Normalized control vs time in the hybrid high-low thrust case

Finally the spacecraft evolution is following represented:

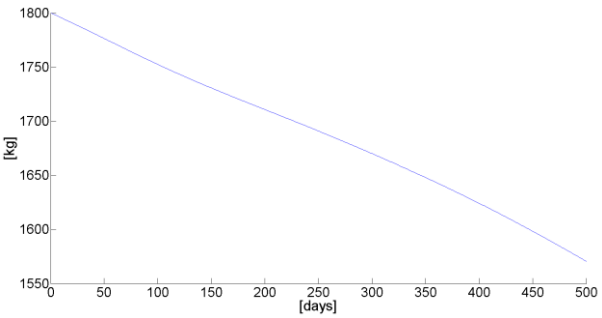

Fig.9: Spacecraft mass vs time in the energy-optimal case

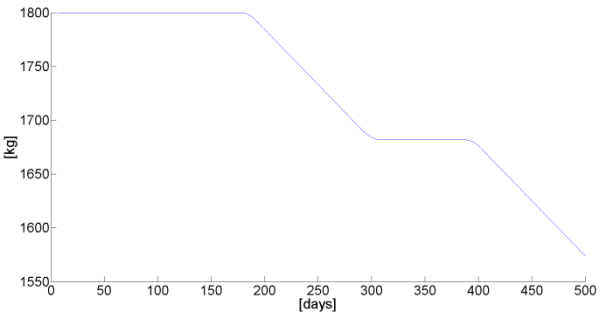

Fig.10: Spacecraft mass vs time in the fuel-optimal case

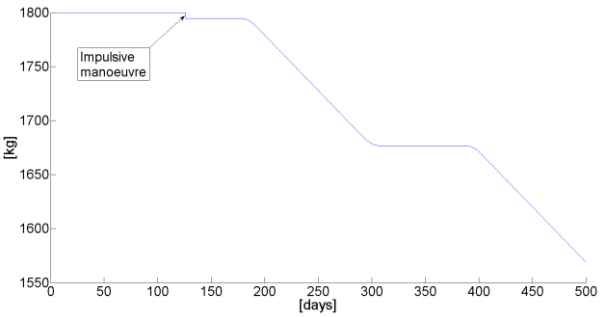

Fig.11: Spacecraft mass vs time in the hybrid high-low thrust case

The validation test case has proven that the optimization algorithm can easily solve simple trajectory optimization problems like the one above illustrated.

However, in the specific test case simulated in order to validate the optimization algorithm developed, it has not be possible to proof an advantage of hybrid high-low thrust propulsion in terms fuel mass consumption. In fact during the third continuation the final spacecraft mass has shown a decreasing trend (meaning a higher fuel mass consumption) following the progressive increase of the impulsive manoeuvre magnitude. The lowest of the increasing values of fuel mass consumption has been assumed at the beginning of the third continuation when the ratio between the final spacecraft mass respectively in the low-thrust and hybrid-thrust case has assumed the value $\mu = \frac{^{(lt)}m(t_f)}{^{(ht)}m(t_f)} = 1.0032$.

V. CONCLUSIONS

The work carried out and illustrated in the present paper has dealt with the development of a framework for general optimization of hybrid-thrust trajectories.

The optimization process makes use of homotopy and numerical continuation in order to compute a fuel-optimal low-thrust trajectory, starting from the solution of a trivial or easy to solve optimization problem. Next, the hybrid-thrust transfer trajectory is computed by including an impulsive manoeuvre to the previously obtained fuel-optimal low-thrust trajectory: this is accomplished by means of a homotopic transformation that links the low-thrust to the hybrid-thrust optimal problem. Subsequently an optimization loop (related to a numerical continuation) progressively increases the impulsive manoeuvre magnitude until the total spacecraft mass is maximized, hence the total fuel mass required for the transfer is minimized.

Although the optimization method developed so far for hybrid-thrust trajectories is still preliminary, numerical test case have been performed in order to validate the software and to start investigating how and when hybrid-thrust propulsion can produce benefits in terms of fuel mass consumption.

Simulation results have shown that the optimization method can easily solve simple trajectory optimization problems, like the one illustrated in this paper. However the preliminary results obtained for the specific test case simulated have not shown an advantage of hybrid high-low thrust propulsion in terms of fuel mass consumption.

If on one hand the optimization algorithm is still at its first development stages and work on its improvement is still in progress, on the other hand it is necessary to underline that several more study cases

need to be simulated and analysed in order to thoroughly investigate the effectiveness of hybrid high-low thrust propulsion. Particularly, it is firstly intended to introduce the hybrid-thrust propulsion in the test cases in which the use of variable specific impulse propulsion (VASIMR) has proven its effectiveness. Since the hybrid high-low thrust propulsion is basically VASIMR pushed to the limit, it is expected that the use of hybrid-thrust propulsion in the same study cases of VASIMR can also give an advantage in terms of fuel mass consumption.

Following the current work, the next steps intended to be performed regard also an enhancement of the generality of the optimization method developed for hybrid-thrust trajectories. This enhancement is intended to be introduced by considering the dynamics equations for the three and subsequently the n-body problem: this can make possible to better investigate the use of hybrid high-low thrust propulsion in a more realistic scenario.

VI. REFERENCES

[Ref.1]: H. Seywald, C. M. Roithmayr, P. A. Troutman, S. Y. Park, *Fuel-Optimal Transfers Between Coplanar Circular Orbits Using Variable-Specific-Impulse Engines*, Journal of Guidance, Control and Dynamics, 2005

[Ref.2]: X. Liang, D. Yang, *Nonplanar Trajectory Optimization with Variable Specific Impulse Engine Using Gauss Pseudospectral Method*, Proceedings of the World Congress on Engineering and Computer Science, 2007

[Ref.3]: C. L. Ranieri, C. A. Ocampo, *Indirect Optimization of Three-Dimensional Finite-Burning Interplanetary Transfers Including Spiral Dynamics*, Journal of Guidance, Control and Dynamics, 2009

[Ref.4]: J.T. Betts, "Practical methods for optimal control and estimation using nonlinear programming (Second edition)", SIAM Advances in Design and Control, 2010.

[Ref.5]: D.G. Hull, "Optimal control theory for applications", Springer, 2003.

[Ref.6]: J.T. Betts, *Survey of numerical methods for trajectory optimization*, Journal of Guidance, Control and Dynamics, 1998.

[Ref.7]: M. Khajehzadeh, M. R. Taha, A. El-shafie, M. Eslami, *A Survey on Meta-Heuristic Global Optimization Algorithms*, Research Journal of Applied Sciences, Engineering and Technology, 2011.

[Ref.8]: T. Haberkorn, P. Martinon, J. Gergaud, *Low-thrust minimum-fuel orbital transfer: a homotopic approach*, Journal of Guidance, Control and Dynamics, 2004.

[Ref.9]: J. Gergaud, T. Haberkorn, *Homotopy method for minimum consumption orbit transfer problem*, ESAIM: Control, Optimisation and Calculus of Variations, 2006.

[Ref.10]: F. Jiang, H. Baoyin, J. Li, *Practical techniques for low-thrust trajectory optimization with homotopic approach*, Journal of Guidance, Control and Dynamics, 2012.

[Ref.11]: F. Topputo, G. Mingotti, F. Bernelli-Zazzera, *Enhancing planetary exploration by using hybrid propulsion transfers*, 63rd International Astronautical Congress, Naples, Italy, 1-5 October 2012, Paper IAC-12-C1.4.3.

[Ref.12]: G. Mingotti, *Parametric study of Earth-to-Moon transfers with hybrid propulsion system and dedicated launch*, Advances in the Astronautical Sciences, 2012.

[Ref.13]: G. Mingotti, F. Topputo, F. Bernelli-Zazzera, *Hybrid propulsion transfers to the moon*, Advances in the Astronautical Sciences, 2012.

[Ref.14]: S. Owens, M. Macdonald, *Novel numerical optimisation of the Hohmann Spiral Transfer*, 64th International Astronautical Congress, Beijing, China, 23-27 September 2013, Paper IAC-13-C1.6.7.

[Ref.15]: H. Curtis, "Orbital mechanics for engineering students", Elsevier Aerospace Engineering Series, 2005.

[Ref.16]: D.A. Vallado, "Fundamentals of Astrodynamics and Applications, 2nd ed. (The Space Technology Library)", Microcosm Inc., 2001.

[Ref.17]: R. H. Battin, "An introduction to the mathematics and methods of astrodynamics - Revised Edition", AIAA Education Series, 1999.

[Ref.18]: M. J. H. Walker, B. Ireland, J. Owens, *A set of modified equinoctial orbit elements*, Celestial Mechanics, 1985.

[Ref.19]: G.W. Whitehead, "Elements of homotopy theory", Springer, 1978.

[Ref.20]: E. L. Allgower, K. Georg, "Numerical Continuation Methods", Springer Series in Computational Mathematics, 1990.